Medicinal chemistry

Abdelrahim et al., Med Chem (Los Angeles) 2016, 6:11
DOI: 10.4172/2161-0444.1000415

Research Article Open Access

Design, Synthesis, Molecular Modelling and Biological Evaluation of Novel α -Naphtholhydroxamate Derivatives as Potential Anticancer Agents

Adel S Abdelrahim[1]*, Syam Mohan[2], Mohamed Albarrati[3], Hafiz Makeen[3] and Safhi MM[4]

[1]*Pharmaceutical Chemistry Department, Faculty of Pharmacy, Al-Azhar University, Cairo, Egypt*
[2]*Medical Research Centre, Jazan University, Saudi Arabia*
[3]*Department of Clinical Pharmacy, Faculty of Pharmacy, Jazan University, Saudi Arabia*
[4]*Department of Pharmacology, Faculty of Pharmacy, Jazan University, Saudi Arabia*

Abstract

Chemotherapy is one of the treatment options for cancer. A major problem in cancer chemotherapy is the lack of selective toxicity of many commonly used anti-cancer agents towards tumor tissue compared to normal tissue. Studies have shown that α-naphthol is selectively toxic to cultures of human tumor tissue compared to normal tissues *in vitro*. Hence, this study was conducted to synthesize a series of new hydroxamate derivatives containing α-naphthol nucleus by the reaction of naphthol acetic acid with amino acid methyl ester derivatives which were directly reacted with hydroxyl amine at room temperature. Structures of these compounds were confirmed by standard studies of IR, ^{1}H NMR, ^{13}CNMR, MS and elemental analysis. The cytotoxicity of the synthesized compounds were studied using the MTT assay in four human cancer cell lines, including HepG2, PC-3, HT-29 and MCF-7. Among the compounds, compound 6_g and 6_h exhibited a significant cytotoxicity against almost all the used cells including the normal cells (WRL-68). Further studies have shown that the cell death observed was closely associated with generation of reactive oxygen species (ROS). In this study, other naphthol derivatives have shown significant increase in the level of ROS in concentration dependent manner in treated cells. In conclusion, the study has shown that among the synthesized compounds, compounds **6_g**, **6_k** and **6_h** hold the potential for further research. Furthermore, a molecular docking of the tested compounds was carried out to investigate their binding pattern with the prospective target, HDAC (PDB-code: 1T69).

Keywords: Chemotherapy; Cancer; Enzyme; Haemoglobin

Introduction

Cancer is one of the major health complications around the globe including United States of America. Presently cancer is the second leading cause of medical death in the US, and is anticipated to exceed heart diseases as the leading cause of death in the coming next few years [1]. According to Council of Health Service breast cancer is the most common cancer among Saudis with 15% of whole reported cancer. In addition classification among sex showed that colorectal cancer is the highest incidence in men, followed by leukaemia and liver. Among the children, leukaemia stands in first place followed by brain and Hodgkin disease [2].

For the last four decades, a number of potential approaches have been proposed for the treatment of cancer. One of the recent targets is Histone deacetylase (HDAC). Modification of histone acetylation level, promoted by HAT and HDAC enzymes, has been recognized to play an important role in the epigenetic modulation of gene expression; in fact this well-known post-translational mechanism is highly involved in the modulation of chromatin plasticity and in the regulation of transcriptional factors accessibility to DNA [3]. Therefore the disruption of histone acetylation pattern is supposed to determine transcriptional disorders and is related to several malignant diseases [4]. Inhibition of HDAC enzyme has proven to induce antiproliferative effects and to promote cellular differentiation. For these reasons, discovery of new agents targeting HDAC enzyme is considered of great interest for the development of anticancer drugs [5].

Hydroxamic acids are among the most well studied compounds due to their significance in so many different applications in modern society. Since it was discovered the first of these acids more than 100 years ago, an extraordinary amount of work has been carried out on the design, preparation, structure-activity relationships (SAR), utilization, and use potential of the hydroxamic acids. These compounds are capable of the inhibition of a variety of enzymes, including ureases, peroxidases, and matrix metalloproteinases. They are also capable of competing as siderophores for iron-(III). In the biomedical sciences, hydroxamic acid moieties are used in the design of therapeutics targeting cancer [6].

The ever-increasing importance of hydroxamic acid functionality in the design of a wide spectrum of bioactive agents, especially of highly potent and selective inhibitors of disease-related metalloproteinases, has heightened the interest in the synthesis of hydroxamic acid-based small molecules [7]. Hydroxamic acids are able to chelate metal ions and therefore inhibit metal-containing enzymes such as matrix metalloproteinases (MMPs). Over expression of MMPs has been linked to a variety of diseases including cancer, rheumatoid arthritis, osteoarthritis and cardiovascular disease [8].

α-Naphthol is selectively toxic to short-term organ cultures of human colonic tumor tissue compared to normal intestinal mucosa taken from the same patients and to human colonic cell lines *in vitro* [9]. 2-Hydroxymethyl-naphthol diacetate, a naphthol derivative, possesses potent cytotoxic activities in human cancer cell lines [9]. Also (+)-3-(2-(2-fluorobenzyloxy) naphthalen-6-yl)-2-aminopropanoic acid derivatives were identified as reversible and competitive protein

***Corresponding author:** Adel S Abdelrahim, Pharmaceutical Chemistry Department, Faculty of Pharmacy (Boys), Al-Azhar University, Cairo, 11884, Egypt, Tel: 25910439; Fax: 25916866; E-mail: dr_adelabdelrahim@yahoo.com

Received November 02, 2016; **Accepted** November 16, 2016; **Published** November 23, 2016

Citation: Abdelrahim AS, Mohan S, Albarrati M, Makeen H, Safhi MM (2016) Design, Synthesis, Molecular Modelling and Biological Evaluation of Novel α-Naphtholhydroxamate Derivatives as Potential Anticancer Agents. Med Chem (Los Angeles) 6: 682-689. doi:10.4172/2161-0444.1000415

tyrosine phosphatases (PTP) inhibitors via a structure-based design approach [9]. 2-Phenylnaphthalenoids derivatives represent a novel type of Top II inhibitory scaffold for developing new antitumor chemotherapeutic agents [10]. Another naphthol derivative has been synthesized and it is found that it is a cell-permeable small molecule inhibitor of KIX–KID interaction, an essential interaction for CREB-dependent gene transcription activation. As a result, this compound is able to inhibit CREB-mediated gene transcription in living cells [11].

Rational of molecular design

Figure 1 showed the basic structural requirements (pharmacophoric features) of histone deacetylase 1 inhibitors; i) Surface recognition Group, ii) Linker group, iii) metal binding group [12]. In addition, it showed some reported histone deacetylase 1 inhibitors with illustration of pharmacophoric features as Vorinostat **I** [13], Panobinostat **II** [14], Belinostat **III** [15], R306465 **IV** [16] and compound **V** [17]. Optimistic by the above observations, we turn our concentration to synthesize a library of novel hybrid compounds comprising hydroxamate moiety with α-naphthol and different linkers of amino acids conjugate. Moreover, chemical modification was carried out to synthesize another series of compounds bearing two hydroxamate moieties. The main core of our design is the investigation of the anticancer activities of these new compounds. Also, we are aiming to study the structure activity relationships (SARs), hoping to obtain more potent anticancer agents.

Experimental

Chemistry

All the chemicals were obtained from Merck, Fluka, Sigma and Aldrich Companies and used without further purification. Melting points were measured using Thermo Fisher Scientific. IR spectra were recorded Bruker tensor 27, FT-IR Spectrophotometer. All ^{1}H NMR

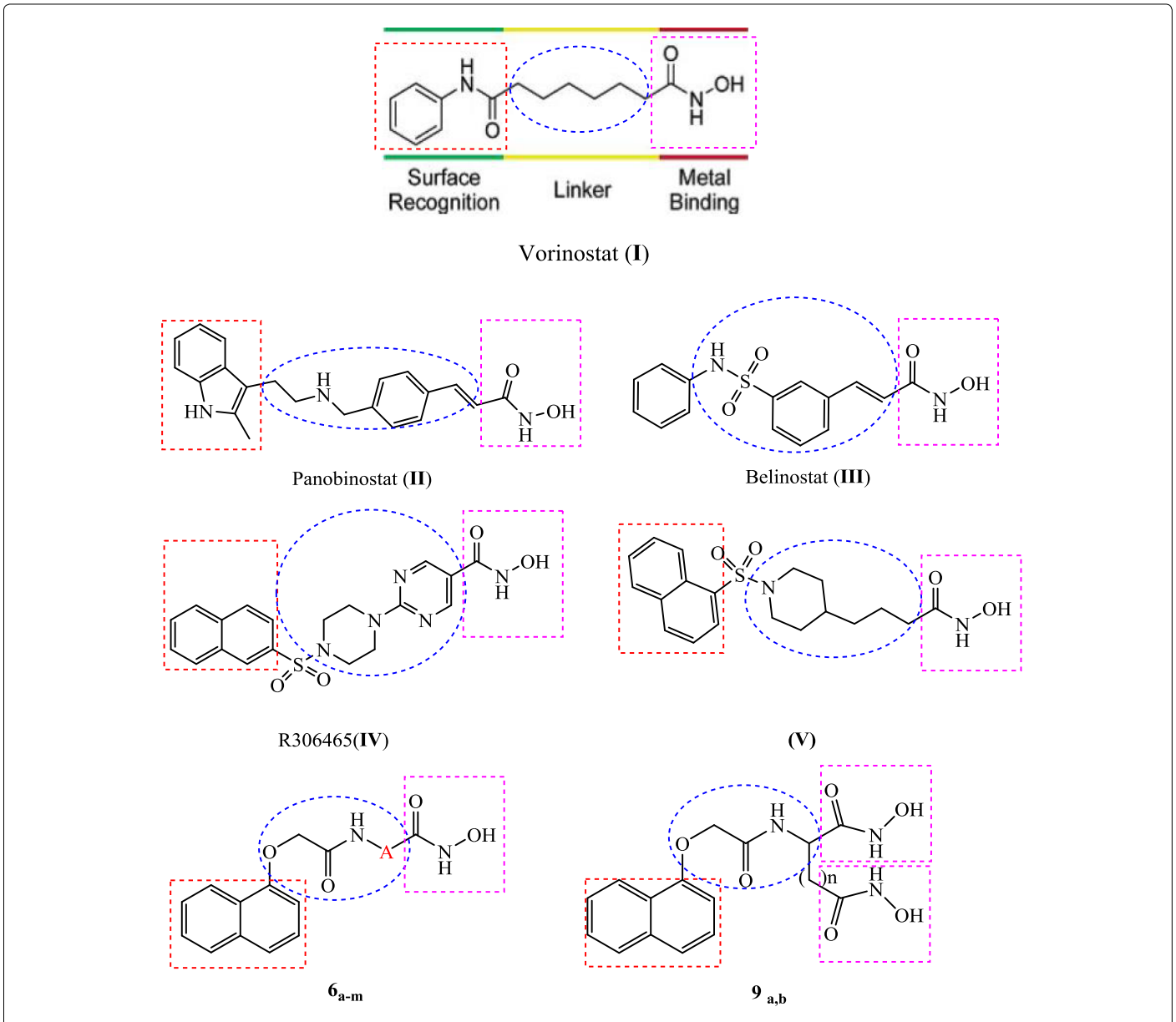

Figure 1: Pharmacophoric features of reported HDAC inhibitors and the synthesized compounds.

spectra were recorded on a Bruker 400 MHz Spectrophotometer. Chemical shifts are reported in parts per million (ppm) using tetramethylsilane (TMS) as an internal standard. Ultraviolet–visible (UV–vis) absorption spectra were recorded on Perkin–Elmer spectrophotometer at the wavelength of maximum absorption (kmax) in a range of DMSO at same concentrations (1×10^{-6} M). The mass Spectra were run on a Shimadzu Qp 5050 Ex Spectrometer. The microanalyses for C, H and N were performed on Perkin–Elmer elemental analyzer.

Naphthol acetic acid (3): α-Naphthol**(1)** (1.44 gm, 10 mmol) was dissolved in dry acetone (50 mL) and then anhydrous potassium carbonate (2.74 gm, 20 mmol) and chloroacetic acid **(2)** (0.94 gm, 10 mmol) were added. The mixture reaction was refluxed overnight and the reaction was checked by TLC. After completion, the reaction mixture was filtered while hot and the solvent was concentrated to produce the title compound **(3)** [9].

Naphthol amino acid methyl ester derivatives (5_{a-m}): Compound **(3)** (1.5 gm, 7 mmol) was refluxed with thionyl chloride (10 mL) for 3 h and the solvent was removed under reduced pressure and the residue was dissolved in dichloromethane (50 mL) and then trimethylamine (3 mL, 30 mmmol) and amino acid methyl ester hydrochloride derivatives **(4)** were added (10 mmol) and the reaction mixture was stirred for 24 h at room temperature. The reaction was checked by TLC and after completion; the reaction mixture was shaken with 5% of hydrochloric acid solution followed by washing with saturated solution of potassium bicarbonate. Then the organic layer was separated, dried using anhydrous magnesium sulphate and evaporated to produce the title compound **(5)** that was used directly without purification.

Naphthol amino acid hydroxamate derivatives (6_{a-m}): Naphthol amino acid methyl ester derivatives **(5_{a-m})** (10 mmol), potassium hydroxide (2.80 gm, 50 mmol.) and hydroxyl amine hydrochloridc (2 gm, 30 mml) were added to dry methanol (50 ml) in ice bath and continuous stirring for 0.5 h and then at room temperature for 12 h. The solvent mixture was removed under vacuum and the residue was dissolved in water and stirred with diethyl ether (2 × 50 mL) and the aqueous layer was separated and acidified with 5% HCl. The precipitate was filtered and recrystallized from methanol to produce the product **(6_{a-m})**.

(i) N-Hydroxy-2-(2-(naphthalen-1-yloxy)acetamido)acetamide (6_a): Yield: 1.15 gm (42%) as a solid; mp 120-123°C. IR (KBr)m: 3300, 3050, 1650 cm^{-1}, ^{1}H NMR ($CDCl_3$, 300 MHz): δ 9.04 (s, NH), 8.34–6.65 (m, 8H), 4.45 (s, 2H, CH_2), 4.00 (s, 2H, CH_2), 2.00 (s, 1H, OH); ^{13}NMR ($CDCl_3$, 300 MHz): δ 168, 166, 156, 134, 127, 126, 120, 66, 39123, 127, 120, MS (EI) m/z: 274.10 (100.0%), 275.10 (15.5%), 276.10 (2.0%). Anal. Calcd for $C_{14}H_{14}N_2O_4$: C, 61.31; H, 5.14; N, 10.21; Found: C, 61.00; 4,98; N, 10.31.

(ii) N-Hydroxy-2-(2-(naphthalen-1-yloxy)acetamido) propanamide (6_b): Yield: 1.64 gm (57%) as a solid; mp 115-116°C. IR (KBr)m: 3300, 3050, 1650 cm^{-1}, ^{1}H NMR ($CDCl_3$, 300 MHz): δ 8.34–6.65 (m, 9H), 4.45 (s, 2H, CH_2), 4.71 (m, 1H, CH), 2.00 (s, 1H, OH), 1.48 (t, 3H, CH_3); ^{13}NMR ($CDCl_3$, 300 MHz): δ 169, 168, 156, 134, 127, 126, 120, 66, 39123, 127, 120, 67, 45, 17; MS (EI) m/z: **:** 288.11 (100.0%), 289.11 (17.0%), 290.12 (2.1%). Anal. Calcd for $C_{15}H_{16}N_2O_4$: C, 62.49; H, 5.59; N, 9.72; Found: C, 62.20; H, 5,50 ; N, 9.89.

(iii) N-Hydroxy-3-(2-(naphthalen-1-yloxy)acetamido) propanamide (6_c): Yield: 1.72 gm (60%) as a solid; mp 130-133 °C. IR (KBr)m: 3300, 3050, 1650 cm^{-1}, ^{1}H NMR ($CDCl_3$, 300 MHz): δ 8.34–6.65 (m, 9H), 4.45 (s, 2H, CH_2), 3.71 (m, 2H, CH_2), 2.66 (m, 2H, CH_2), 2.00 (s, 1H, OH); ^{13}NMR ($CDCl_3$, 300 MHz): δ 169, 168, 156, 134, 127, 126, 120, 66, 39123, 127, 120, 67, 45, 42, 37; MS (EI) m/z: **:** 288.11 (100.0%), 289.11 (17.0%), 290.12 (2.1%). Anal. Calcd for $C_{15}H_{16}N_2O_4$: C, 62.49; H, 5.59; N, 9.72; Found: C, 62.32; H, 5,65 ; N, 9.85.

(iv) N-Hydroxy-3-mercapto-2-(2-(naphthalen-1-yloxy) acetamido)propanamide (6_d): Yield: 0.9 gm (28%) as a solid; mp 105-108 °C. IR (KBr)m: 3300, 3050, 1650 cm^{-1}, ^{1}H NMR ($CDCl_3$, 300 MHz): δ 8.34–6.65 (m, 9H), 4.67 (s, 2H, CH_2), 4.54 (m, 1H, CH), 2.66 (m, 2H, CH_2), 2.00 (s, 1H, OH), 1.49 (s, 1H, SH);; ^{13}NMR ($CDCl_3$, 300 MHz): δ 169, 168, 156, 134, 127, 126, 120, 66, 39123, 127, 120, 67, 45, 37; MS (EI) m/z: 320.08 (100.0%), 321.09 (16.6%), 322.08 (4.6%), 322.09 (2.2%), 321.08 (1.5%). Anal. Calcd for $C_{15}H_{16}N_2O_4S$ C, 56.24; H, 5.03; N, 8.74; Found: C, 56. 18; H, 4,93 ; N, 8.64.

(v) N-Hydroxy-4-methyl-2-(2-(naphthalen-1-yloxy)acetamido) pentanamide (6_e): Yield: 1.70 gm (51%) as a solid; mp 125-128 °C. IR (KBr)m: 3300, 3050, 1650 cm^{-1}, ^{1}H NMR ($CDCl_3$, 300 MHz): δ 8.34–6.65 (m, 9H, Ar, 2NH), 4.92 (m, 3H, CH, CH_2), 2.00 (s, 1H, OH), 1.76 (m, 2H, CH_2), 1.46 (m, 1H, CH), 0.89 (m, 6H, $2CH_3$), ^{13}NMR ($CDCl_3$, 300 MHz): δ 169, 168, 156, 134, 127, 126, 120, 66, 45, 37; MS (EI) m/z: 330.16 (100.0%), 331.16 (19.9%), 332.16 (2.8%). Anal. Calcd for $C_{18}H_{22}N_2O_4$; C, 65.44; H, 6.71; N, 8.48; Found: C, 65.39, H, 6.83; N, 8.54.

(vi) N-Hydroxy-1-(2-(naphthalen-1-yloxy)acetyl)pyrrolidine-2-carboxamide (6_f): Yield: 0.94 gm (30%) as a solid; mp 105-107 °C. IR (KBr)m: 3300, 3050, 1650 cm^{-1}, ^{1}H NMR ($CDCl_3$, 300 MHz): δ 8.34–6.65 (m, 8H, Ar,1NH), 4.83 (s, 2H, CH_2), 4.22-2.54 (m, 7H, 1CH, $3CH_2$), 2.00 (s, 1H, OH); ^{13}NMR ($CDCl_3$, 300 MHz): δ 169, 168, 156, 134, 127, 126, 120, 66, 39123, 127, 120, 67, 45, 29, 21; MS (EI) m/z: 314.13 (100.0%), 315.13 (18.7%), 316.13 (2.6%):. Anal. Calcd for $C_{17}H_{18}N_2O_4$ C, 64.96; H, 5.77; N, 8.91; Found C, 64.92, H, 5.96; N, 8.85.

(vii) N-Hydroxy-2-(2-(naphthalen-1-yloxy)acetamido)-3-phenylpropanamide (6_g): Yield: 1.4 gm (38%) as a solid; mp 132-135 °C. IR (KBr)m: 3300, 3050, 1650 cm^{-1}, ^{1}H NMR ($CDCl_3$, 300 MHz): δ 8.34–6.65 (m, 14H, Ar,2NH), 4.92 (m, 3H, CH, CH_2), 3.44-3.25 (m, 2H, CH_2), 2.00 (s, 1H, OH); ^{13}NMR ($CDCl_3$, 300 MHz): δ 169, 168, 158, 134, 133, 127, 126, 125, 124, 120, 107, 67, 49, 37; MS (EI) m/z: 364.14 (100.0%), 365.15 (23.1%), 366.15 (3.4%)). Anal. Calcd for $C_{21}H_{20}N_2O_4$: C, 69.22; H, 5.53; N, 7.69; Found C, 69.10, H, 5.45; N, 7.75.

(viii) N-Hydroxy-3-(4-hydroxyphenyl)-2-(2-(naphthalen-1-yloxy)acetamido)propanamide (6_h): Yield: 1.2 gm (31%) as a solid; mp 115-117 °C. IR (KBr)m: 3300, 3050, 1650 cm^{-1}, ^{1}H NMR ($CDCl_3$, 300 MHz): δ 9.43 (s, 1H, OH), 8.31–6.65 (m, 13H, Ar,2NH), 4.85 (m, 3H, CH, CH_2), 3.44-3.19 (m, 2H, CH_2), 2.00 (s, 1H, OH); ^{13}NMR ($CDCl_3$, 300 MHz): δ 169, 168, 158, 155, 134, 130, 129, 126, 125, 124, 120, 115, 107, 67, 49, 37; MS (EI) m/z: 380.14 (100.0%), 381.14 (23.1%), 382.14 (3.7%). Anal. Calcd for: $C_{21}H_{20}N_2O_5$: C, 66.31; H, 5.30; N, 7.36; Found C, 66.20, H, 5.18; N, 7.45.

(ix) N-Hydroxy-3-(1H-indol-3-yl)-2-(2-(naphthalen-1-yloxy) acetamido)propanamide (6_i): Yield: 1. gm (25%) as a solid; mp 125-127 °C. IR (KBr)m: 3300, 3050, 1650 cm^{-1}, ^{1}H NMR ($CDCl_3$, 300 MHz): δ 10.65 (s, 1H, NH), 8.31–6.65 (m, 14H, Ar,2NH), 4.92 (m, 3H, CH, CH_2), 3.44-3.25 (m, 2H, CH_2), 2.00 (s, 1H, OH); ^{13}NMR ($CDCl_3$, 300 MHz): δ 168, 158, 134, 127, 126, 124, 120, 118, 111, 109, 107, 67, 49, 27; MS (EI) m/z: 403.15 (100.0%), 404.16 (25.3%), 405.16 (3.9%), 404.15 (1.1%). Anal. Calcd for : $C_{23}H_{21}N_3O_4$: C, 68.47; H, 5.25; N, 10.42; Found C, 68.50, H, 5.30; N, 10.35.

(x) N1-Hydroxy-2-(2-(naphthalen-1-yloxy)acetamido) succinamide (6_j): Yield: 1.7 gm (49%) as a solid; mp 120-123 °C. IR (KBr)m: 3300, 3050, 1650 cm^{-1}, ^{1}H NMR ($CDCl_3$, 300 MHz): δ 8.31–6.65

(m, 10H, Ar,3NH), 4.92 (m, 3H, CH, CH_2), 2.36 (m, 4H, $2CH_2$), 2.00 (s, 1H, OH); ^{13}NMR ($CDCl_3$, 300 MHz): δ 172, 169, 168, 156, 134, 127, 126, 124, 123, 120, 107, 67, 46, 30; MS (EI) m/z: 331.12 (100.0%), 332.12 (17.7%), 333.12 (2.7%), 332.11 (1.1%). Anal. Calcd for: $C_{16}H_{17}N_3O_5$: C, 58.00; H, 5.17; N, 12.68; Found C, 58.25, H, 5.05; N, 12.59.

(xi) N1-Hydroxy-2-(2-(naphthalen-1-yloxy)acetamido) pentanediamide (6_k): Yield: 1.5 gm (43%) as a solid; mp 130-133 °C. IR (KBr)m: 3300, 3050, 1650 cm^{-1}, ^{1}H NMR ($CDCl_3$, 300 MHz): δ 8.31–6.65 (m, 10H, Ar,3NH), 4.92 (m, 3H, CH, CH_2), 2.25 (m, 4H, $2CH_2$), 2.00 (s, 1H, OH); ^{13}NMR ($CDCl_3$, 300 MHz): δ 173, 169, 168, 156, 134, 127, 126, 124, 123, 120, 107, 67, 49, 32, 27; MS (EI) m/z: 345.13 (100.0%), 346.14 (18.8%), 347.14 (2.7%), 346.13 (1.1%). Anal. Calcd for: $C_{17}H_{19}N_3O_5$: C, 59.12; H, 5.55; N, 12.17; Found C, 59.05, H, 5.45; N, 12.25.

(xii) 4-(Hydroxyamino)-3-(2-(naphthalen-1-yloxy)acetamido)-4-oxobutanoic acid (9_a): Yield: 1.4 gm (42%) as a solid; mp 105-107 °C. IR (KBr)m: 3300, 3050, 1650 cm^{-1}, ^{1}H NMR ($CDCl_3$, 300 MHz): δ 12.54 (s, 1H, COOH), 8.31–6.65 (m, 9H, Ar,2NH), 4.92 (m, 3H, CH, CH2), 3.44-3.19 (m, 2H, CH_2), 2.00 (s, 1H, OH); ^{13}NMR ($CDCl_3$, 300 MHz): δ 173, 168, 165, 156, 127, 126, 124, 109, 107, 67, 49, 37; MS (EI) m/z: 332.10 (100.0%), 333.10 (18.0%), 334.11 (2.7%). Anal. Calcd for: $C_{16}H_{16}N_2O_6$: C, 57.83; H, 4.85; N, 8.43; Found C, 57.70, H, 5.90; N, 8.36.

(xiii) 5-(Hydroxyamino)-4-(2-(naphthalen-1-yloxy)acetamido)-5-oxopentanoic acid (9_b): Yield: 1.7 gm (49%) as a solid; mp 120-123 °C. IR (KBr)m: 3300, 3050, 1650 cm^{-1}, ^{1}H NMR ($CDCl_3$, 300 MHz): δ 12.12 (s, 1H, COOH), 8.31–6.65 (m, 9H, Ar,2NH), 4.92 (m, 3H, CH, CH_2), 2.25 (m, 4H, $2CH_2$), 2.00 (s, 1H, OH); ^{13}NMR ($CDCl_3$, 300 MHz): δ 176, 168, 156, 134, 127, 126, 124, 107, 67, 30, 26; MS (EI) m/z: 346.12 (100.0%), 347.12 (18.8%), 348.12 (3.0%). Anal. Calcd for: $C_{17}H_{18}N_2O_6$: C, 58.96; H, 5.24; N, 8.09; Found C, 59.00, H, 5.30; N, 8.15.

Biological evaluation

Cell culture and cell viability: Hepg2, PC3, HT29, MCF 7, and WRL68 cells were obtained from ATTC. The RPMI-1640 medium, which is supplemented with 10% foetal bovine serum (FBS) and 1% penicillin and streptomycin were used in a humidified conditions at 5% CO_2 and 37°C.

MTT assay has been used to measure the viability of percentage of cells upon treatments with various compounds under investigation [18]. Briefly, cells (5×10^4 cells/ml) were treated with compounds at different concentration in 96-well plate and incubated for 24 h. Compounds were then diluted in various concentrations and treated for another 24 hours. The end point colour developed was measured and recorded at absorbance of 570 nm using Eliza reader. Raw data of absorbance were used to calculate results which were expressed as percentage of control giving percentage cell viability after 24 h exposure to test agent. The potency of cell growth inhibition for test agent was expressed as IC_{50} value.

Intracellular ROS level: Since the compound 6_g and 6_h were exhibited significant cytotoxicity, only these compounds were used to detect the level of ROS in HepG2 cells. 2′,7′-dichlorluorescin diacetate (DCFH-DA) was used to measure the production of intracellular ROS according to reported procedure [19]. In brief, DCFH-DA stock solution (10 mM) was diluted 500-fold in Hank's Balanced Salt Solution (HBSS) to yield a working solution of 20 μM. After 24 h of exposure to compounds the cells in the 96- well black plate was washed twice with HBSS and then incubated in 100 μl working solution of DCFH-DA at 37°C for 30 min. Fluorescence was then determined at 485-nm excitation and 520 nm emission using a fluorescence microplate reader.

Hemolytic assays: The interaction between the synthesized compounds 6_g, 6_h and 6_k with erythrocyte membranes was investigated using hemolytic experiments. Hemolysis was used to quantify the membrane-damaging properties of compounds 6_g, 6_h and 6_k. Human erythrocytes were isolated from fresh heparin-treated blood collected from healthy adult volunteers by centrifugation at 3000 rpm for 15 min (Sigma 2-5 centrifuge, Sigma Laborzentrifugen GmbH, Osterode am Harz, Germany). The pellet was washed four times with an isotonic phosphate buffer saline (PBS) at pH 7.4, centrifuged at 3000 rpm for 15 min and resuspended in the same buffer. The erythrocyte pellet was diluted in PBS at pH 7.4 to a final concentration of 4% (v/v) erythrocytes. This stock solution was always freshly prepared and used within 24 h.

Compounds 6_g, 6_h and 6_k were prepared in PBS at different concentrations (0.1, 0.5, 1, 5 and 10 mM) and transferred to 96-well flat-bottom microtiter plates (TPP, Zurich, Switzerland). The plates were then incubated at 37°C for 60 min on a Titramax 1000 Vibrating Shaker (Heidolph, Schwabach, Germany). Erythrocyte suspensions (100 μl) were added to each well on the plate and incubated for 60 min at 37°C with constant shaking. After centrifugation at 3000 rpm for 15 min, the release of hemoglobin was determined by photometric analysis of the supernatant at 540 nm. Complete hemolysis was achieved by using 10 mM of sodium dodecyl sulfate (SDS) in PBS as a positive control (100%), while PBS was used as a negative control. Each experiment was performed in triplicate. The percentage of hemolysis was calculated according to the following formula:

$$\%\text{lysis} = \left[\frac{A_{test} - A_{blank}}{A_{100\%lysis} - A_{blank}}\right] \times 100 \quad (1)$$

where A_{test} is the absorbance value of the hemoglobin released from erythrocytes treated with the test compounds; A_{blank} is the absorbance value of the hemoglobin released from erythrocytes treated with PBS buffer, and $A_{100\%lysis}$ is the absorbance value of the hemoglobin released from erythrocytes treated with 10 mmol SDS in PBS solution [20].

Molecular docking studies

Molecular docking studies were carried out using AutoDock 4.2 [21] tool to predict the preferred binding mode and binding sites of synthesized compounds with the crystal structure of the HDAC8. The structures of the synthesized compounds were drawn using ACD/ChemSketch and its geometry was optimized by combine use of Gaussian 03 program and Autodock 4.2. The crystal structure of HDAC8 (PDB ID: 1T69) was obtained from Protein Data Bank, www.rcsb.org/pdb/home/home.do. Before docking analysis Hetatm were removed from the protein and the energy was minimized using SPDBV-Swiss-pdbviewer. For docking calculations, the receptor file prepared with the addition of polar hydrogens, Kollman charges, and solvation parameters. The precalculated grid maps set at the size set at 60, 60, and 60 A° (x, y, and z) to include all the amino acid residues that present in the receptor. The spacing between grid points was 0.575 angstroms. The Lamarckian genetic algorithm (LGA) chosen to confirm maximum of 10 conformers was considered to the docking process with the population size of 150 individuals. The output from AutoDock was further analyzed with PyMOLoftware package [9].

Results and Discussion

Chemistry

The newly synthesized compounds were designed by joining two different moieties as mentioned in Scheme 1. α-Naphthol was reacted with chloroacetic acid to afford 2-(naphthalen-1-yloxy)acetic acid **3**

and subsequent reacted with amino acid methyl ester hydrochloride derivatives to give the corresponding compounds $\mathbf{5}_{(a\text{-}m)}$. The obtained derivatives were reacted with hydroxyl amine hydrochloride in freshly distilled methanol to prevent any moisture that harms the presence of ester with potassium hydroxide. Also, the reaction was accomplished at room temperature to prevent also ester hydrolysis. By exploiting this technique, the yield was satisfactory (Scheme 1).

Also, aspartic and glutamic acids were used to synthesis compounds bearing two hydroxamate moieties to examine the effect of two hydroxamate moieties on the biological activities as in Scheme 2.

Biological evaluation

Cell culture and cell viability: *In vitro* cell assay is the best method to screen the ability of synthetic compounds against various cancers. Using these cells, many cytotoxicity assays has been developed. The significant one is the colorimetric MTT assay, which is based on the assumption that dead cells or their products do not reduce tetrazolium [22]. The assay depends both on the number of cells present and on the mitochondrial activity per cell. In the current study, the cytotoxicity of the synthesized compounds were studied using the MTT assay in four human cancer cell lines, including Hepg2, PC3, HT29, MCF 7, and WRL68. The results are listed in Table 1.

The different cell lines were selected due to some considerations. i) Hepatocellular carcinoma (HCC) is now the third leading cause of cancer deaths worldwide, with over 500,000 people affected. The incidence of HCC is highest in Asia and Africa, where the endemic high prevalence of hepatitis B and hepatitis C strongly predisposes to the development of chronic liver disease and subsequent development of HCC [23]. ii) The selected cell lines cover the most common cancer diseases.

Among the compounds, compound $\mathbf{6}_g$ had exhibited significant cytotoxicity against almost all the used cells including the normal cells. The next significant compound which showed cytotoxicity was compound $\mathbf{6}_i$ that showed significant cytotoxicity against almost all the used cells including the normal cells but less than compound $\mathbf{6}_g$. Compound $\mathbf{6}_h$ was showed cytotoxicity to Hepg2 cells alone with an IC_{50} of 7.1 ± 0.4 μM.

Intracellular ROS level: The cell death and ROS generation is closely associated [24]. Reactive oxygen species (ROS) are emerging as critical signalling molecules. The term reactive oxygen species encompasses a wide range of molecules. Free radicals are chemical species containing one or more unpaired electrons [25]. Therapeutic strategies that promote ROS accumulation and cell death have been explored based on the availability of drugs that interfere with scavenging. Hence the Intracellular ROS was measured in HepG2 cells with 10 and 20 μg/ml concentrations of compound $\mathbf{6}_g$ and $\mathbf{6}_h$. As the Figure 1A and 1B showed both the compounds has exhibited significant increase in the level of ROS in concentration dependent manner in treated cells (Figure 2).

Hemolytic assay: The release of hemoglobin was used to quantify the membrane damaging properties of the synthesized compounds. Erythrocytes were treated with PBS and SDS to obtain values corresponding to 0 and 100% of lysis, respectively [25]. The erythrocytes were incubated for 1 h with five different concentrations (0.1, 0.5, 1, 5 and 10 mM of compounds $\mathbf{6}_g$, $\mathbf{6}_h$ and $\mathbf{6}_k$ to measure hemolyticlysis. Only compound $\mathbf{6}_g$ with higher concentration (10mM showed significant hemolysis due to higher lipophilicity characteristics. while compounds $\mathbf{6}_h$ and $\mathbf{6}_k$ caused almost no hemolysis (≤ 10%) even in higher concentration. These results correlate with our prediction using mollinspiration data base.

Molecular docking studies

In order to get preliminary information on the binding mode of these compounds to HDAC, we selected three representative compounds, $\mathbf{5}_g$, $\mathbf{5}_h$, and $\mathbf{6}_k$ which showing the highest affinity for docking study. Since crystal structures of HDAC3 and HDAC4 in complex with SAHA have not been determined so far, we used the crystal structure of HDAC8 in complex with SAHA which shows sequence similarity (46%) to HDAC4 [1], for docking experiments of compound $\mathbf{5}_g$, $\mathbf{5}_h$, and $\mathbf{6}_k$. We implemented control docking experiments with SAHA to the crystal structure of HDAC8 using AutoDock program [26,27].

The proposed binding mode of compound $(\mathbf{6}_g)$ is that the phenyl ring of the compound 6g is involved in aromatic stacking interactions with Phe152, His143, His180, His208, and Tyr306. The two amino groups of the compound is involved in a hydrogen bonding interaction with Asp101. The bicyclic moiety of the compound is involved in aromatic stacking interactions with Tyr100 and Tyr306 and is located in the hydrophobic pocket formed by Ile34, lyophobic part of Lys33, and Met274 (Figure 3), and because of the existence of additional hydrogen bonding, desirable interactions, and can nicely fit into the binding site, compound $(\mathbf{6}_g)$ has the highest affinity towards the receptor than other compounds showing anticancer activity towards Hepg-2, PC-3, HT-

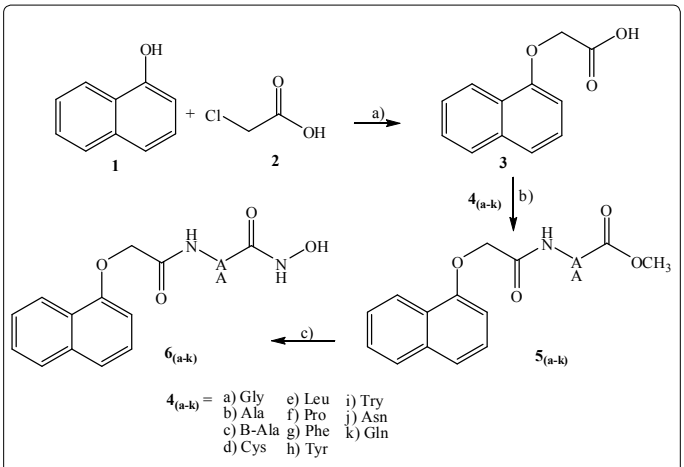

Scheme 1: Reagents and conditions: a) K_2CO_3, acetone 70°C, 12 h; b) (i) $SOCl_2$, DCM, reflux 3 h, rt, (ii) amino acid methyl ester hydrochloride **4**, TEA, DCM, rt, 24 h; c) NH_2OH, KOH, CH_3OH, rt, 12 h.

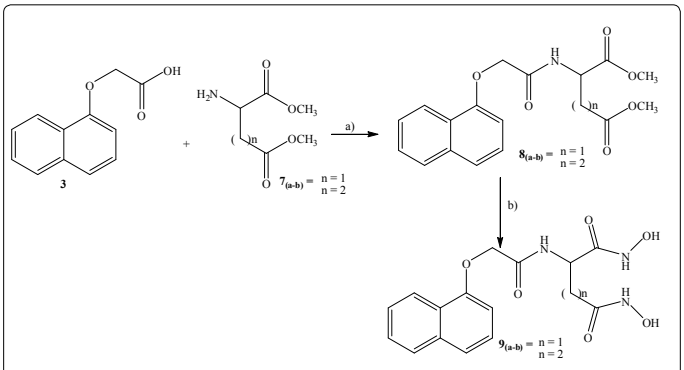

Scheme 2: Reagents and conditions: a) (i) $SOCl_2$, DCM, reflux 3 h, rt, (ii) amino acid methyl ester hydrochloride **7**, TEA, DCM, rt, 24 h; b) NH_2OH, KOH, CH_3OH, rt, 12 h.

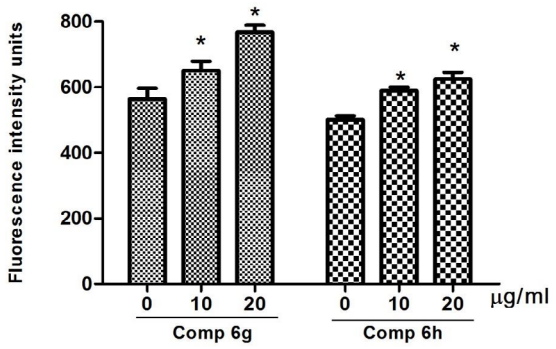

Figure 2: Effects of Compound 6g and 6h on HepG2 cells ROS generation. DCF-fluorescence intensity after 10 and 20 µg/ml of exposure at 24 h. Values are mean ± SD from three independent experiments. Triplicates of each treatment group were used in each independent experiment. The Statistical significance is expressed as *P<0.05.

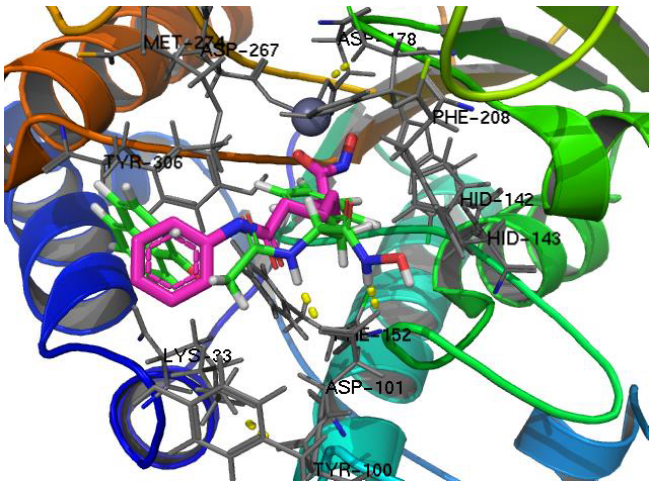

Figure 3: Predicted binding modes of compound $\mathbf{6}_g$ to HDAC8. The actual binding pose of SAHA to HDAC8 is shown as a stick model with carbon colored in magenta, and compound 6g colored in green. Nitrogen in blue, and oxygen in red. The important residues for the interaction are colored in gray. Other atoms are colored same as Zn^{2+} ion is shown as a dark gray sphere.

29, MCF-7 and WRL-68 cell lines with IC_{50} value of 8.2, 16.1, 14.3, 13.6 and 6.5 µgM, respectively.

On the other hand, compound ($\mathbf{6}_h$) exhibited promising anticancer activity towards Hepg-2, PC-3, HT-29, MCF-7 and WRL-68 cell lines with IC_{50} value of 9, 12.1, 49.0, and 61.0 µg/ml, respectively. Thus, introduction of hydroxyl group attached with the phenyl moiety of the compound ($\mathbf{6}_h$) is likely important for increasing the affinity for the receptor. The obtained result for compound ($\mathbf{6}_h$) is virtually the same as that of compound ($\mathbf{6}_g$). In addition, the hydroxyl group is stabilized by a hydrogen bonding interaction with Tyr306. However, the one amino group is only involved in a hydrogen bonding interactions Asp101 which can decrease the affinity for the receptor (Figure 4).

Whereas, compound ($\mathbf{6}_i$) exhibited significant anticancer activity towards WRL-68, Hepg-2, MCF-7, PC-3, and HT-29 cell lines with IC_{50} value of 7.1, 20.6, 21.2, 18.0, and 9.0 µM, respectively. The obtained results were explained and confirmed by docking modeling data where, the obtained binding mode of compound ($\mathbf{6}_k$) with the binding site of HDAC8 follows the general pattern observed for compound ($\mathbf{6}_g$). As before, the hydrogen bonding interactions and aromatic stacking interactions are maintained. However, insertion of indole moiety of the compound $\mathbf{6}_i$ could abolish aromatic stacking interaction with Tyr100 which is essential for ligand affinity. Furthermore, due to desirable interactions compound cannot accommodate the binding site (Figure 5).

ADME profiling

The bioavailability of these compounds can be predicted using mipc-Molinspiration Property Calculator [28]. In particular, we calculated the compliance of compounds to Lipinski's "rule of five" to evaluate the drug-likeness [29]. The rule describes molecular properties which are important for drug's pharmacokinetics in the human body, including their absorption, distribution, metabolism and elimination (ADME) and it is used to make sure that drug like physicochemical properties are maintained during drug design. This simple rule states that orally active drug has no more than one violation of the following criteria: molecular weight less than 500 Dalton; no more than five hydrogen bond donors; no more than 10 hydrogen bond acceptors; and calculated octanol–water partition coefficient (mlogP) not greater than 5 [30]. Moreover, topological polar surface area (TPSA) together with the number of rotatable bonds have been considered to be very good descriptors of oral bioavailability of drugs. Compounds which meet the following two criteria: ten or fewer rotatable bonds and polar surface area equal to or less than 140 $Å^2$ are predicted to exhibit good oral bioavailability. The calculated parameters presented in Table showed good bioavailability of studied compounds.

The most active compounds $\mathbf{6}_g$, $\mathbf{6}_h$ and $\mathbf{6}_k$ fulfilled all rules. Theoretically, these three compounds should exhibit good passive oral absorption and differences in their bioactivity cannot be attributed to these properties. Also, the determined logP values were 2.84, 2.36 and 0.31 respectively, which affirmed the hydrophilic-lipophilic balance of compounds $\mathbf{6}_g$ and $\mathbf{6}_h$ while compound $\mathbf{6}_k$ is more hydroophilic and consequently more water solubility (Table 2).

SAR

Observing the results, we could deduce valuable data about the structure activity relationships. Firstly, we explored the effect of amino acid linkers. The decreased IC_{50} values of compounds $\mathbf{6}_f$, $\mathbf{6}_g$, $\mathbf{6}_i$, **and** $\mathbf{6}_j$ with incorporated Phe, Tyr and Gln moieties, respectively than those of their corresponding members indicated that substitution with Phe, Tyr and Gln is advantageous.

We then investigated the impact of the substitution with two hydroxamate moieties. It was found that the insertion of two hydroxamate moieties is more preferred biologically. Moreover, the substitution with glutamate moiety is more advantageous than that of aspartate one

Conclusion

To sum up, in the present study we have described a straightforward and efficient synthesis of thirteen novel hybrid compounds containing hydroxamate moiety with α-naphthol amino acid conjugates, starting from simply prepared α-naphthol amino acid esters. The biological activities and structure-activity relationships (SARs) of the newly synthesized compounds were evaluated. Using hydroxamic acid with potassium hydroxide at room temperature for long period was found beneficial than using potassium hydroxide with heating because it hydrolyzed amino acid ester before the reaction. In Addition using different derivatives of amino acids (lipophilic and hydrophilic) helps us to study structure activity relationships of these derivatives and

Comp.	IC_{50} (μM)[a]					ΔG[c] kcal/mol
	HePG2	PC3	HT29	MCF-7	WRL68	
6_a	NA[b]	NA[b]	NA[b]	NA[b]	NA[b]	- 20.91
6_b	NA[b]	NA[b]	NA[b]	NA[b]	81.6 ±1.1	- 30.30
6_c	11.7 ± 1.3	22.0 ± 1.9	40.8 ± 2.71	21.6 ± 2.8	11.2 ± 1.1	- 30.17
6_d	12.8 ± 1.4	29.9 ± 1.5	43.6 ± 2.4	22.5 ± 1.7	9.2 ± 1.3	- 30.23
6_e	NA[b]	NA[b]	NA[b]	NA[b]	15.6 ± 5.3	- 40.89
6_f	15.8 ± 1.5	30.0 ± 1.6	45.0 ± 1.1	30.8 ± 1.9	12.5 ± 2.2	- 30.72
6_g	8.2 ± 1.1	16.1 ± 1.3	14.3± 0.8	13.6 ± 1.1	6.5 ± 2.3	- 50.92
6_h	7.1 ± 0.4	20.6 ± 1.7	21.2 ± 1.2	18.0 ± 0.9	9.0 ± 1.2	- 50.84
6_i	7.8 ± 0.7	21.4 ± 1.3	19.2 ± 1.3	16.8 ± 3.6	4.6 ± 1.2	- 50.36
6_j	15.6 ± 1.7	28.4 ± 1.1	NA[b]	44.8 ± 2.7	5.9 ± 4.3	- 40.48
6_k	16.9 ± 2.0	26.3± 3.1	46.8 ± 1.7	26.3 ± 1.7	8.7 ± 3.1	- 50.07
9_a	29.1 ± 1.4	16.9 ± 1.3	NA[b]	30.3 ± 1.3	19.4 ± 2.2	- 40.61
9_b	24.1 ± 0.9	26.3 ± 1.8	33.2± 0.1	27.7± 2.3	15.0 ± 4.2	- 40.61
Doxo[d]	5.76 ± 0.4	8.22 ± 1.2	6.13 ± 2.0	7.73 ±1.1	4.54 ± 1.4	NT[f]
SHH[e]	NT[f]	NT[f]	NT[f]	NT[f]	NT[f]	- 55.23

[a]IC_{50} values are the mean ± SD of three separate experiments; [b]NA: Compounds having IC_{50} value >50 μM; [c]Docking energy scores; [d]Doxo: Doxorubicin; [e]SHH: co-crystallized ligand (*Octanedioic acid hydroxyamidephenylamide*); [f]NT: Compounds not tested.

Table 1: IC_{50} values of compounds in selected cell lines assessed by MTT assay.

Comp.	MW	No. of H-bond donors	No. of H-bond acceptors	milogP	No. of rotatable bonds	TPSA	No. of violation
6_a	274.28	3	6	1.05	5	87.66	0
6_b	288.30	3	6	1.38	5	87.66	0
6_c	288.30	3	6	1.32	6	87.66	0
6_d	320.37	3	6	1.36	6	87.66	0
6_e	330.38	3	6	2.69	7	87.66	0
6_f	314.34	2	6	1.68	4	78.87	0
6_g	364.40	3	6	2.84	7	87.66	0
6_h	380.40	4	7	2.36	7	107.89	0
6_i	403.44	4	7	2.99	7	103.45	0
6_j	331.33	5	8	1.26	7	130.75	0
6_k	345.36	5	8	0.31	8	130.75	0
9_a	347.33	5	9	1.32	7	136.98	0
9_b	361.35	5	9	0.37	8	136.98	0

MW: Molecular weight; milogP: Octanol-water partition coefficient (logP predicted at Molinspiration); TPSA: Topological polar surface area

Table 2: ADME of synthesized compounds 6_{a-k} and 9_{a-b} using Molinspiration property calculator.

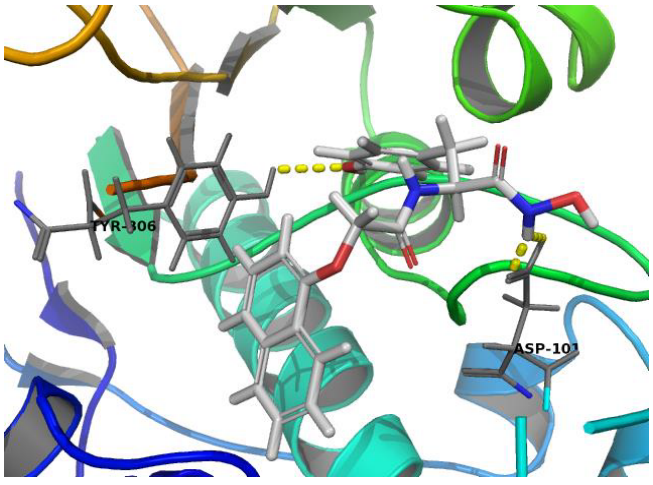

Figure 4: Predicted binding modes of compound 6_h to HDAC8. The actual binding pose of 6_h to HDAC8 is shown as a stick model with carbon colored in grey. Nitrogen in blue, and oxygen in red.

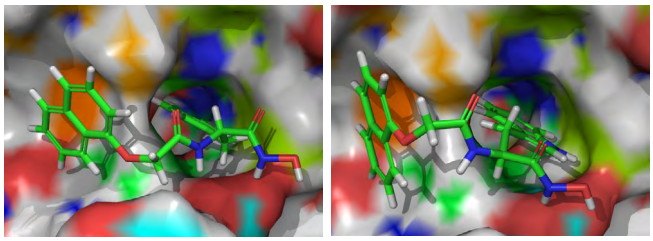

Figure 5: View of surface and active site of compounds 6_g and 6_k bound to HDAC8. Compound (6_g) can fit nicely inside the binding pocket.

encouraged us to make more modification to find out more effective and safer derivatives. The docking studies also supported the results concluded from the anti-proliferation screening. The results of this study may find a lead toward the development of new therapeutic agent to fight cancer. But all these findings support the need for further investigations such as molecular optimization, enzymatic assay and *in vivo* studies of more effective compound may be considered a future plan for producing effective and safer anticancer agents.

Citation: Abdelrahim AS, Mohan S, Albarrati M, Makeen H, Safhi MM (2016) Design, Synthesis, Molecular Modelling and Biological Evaluation of Novel α-Naphtholhydroxamate Derivatives as Potential Anticancer Agents. Med Chem (Los Angeles) 6: 682-689. doi:10.4172/2161-0444.1000415

Acknowledgements

The authors wish to express their thanks to Dr. Mohamed Elsafhi, Dean of the Faculty of Pharmacy, Jazan University for his help.

References

1. Panneerselvam P, Nair RR, Vijayalakshmi G, Subramanian EH, Sridhar SK (2005) Synthesis of schiff bases of 4-(4-aminophenyl)-morpholine as potential antimicrobial agents. European journal of medicinal chemistry 40: 225-229.
2. Gomez CM, Kouznetsov V (2013) Recent developments on antimicrobial quinoline chemistry. Formatex 1: 666-677.
3. Van Beusichem M, Farrell N (1992) Activation of the trans geometry in platinum antitumor complexes. Synthesis, characterization, and biological activity of complexes with the planar ligands pyridine, n-methylimidazole, thiazole, and quinoline, Crystal and molecular structure of trans-dichlorobis (thiazole) platinum (iii). Inorganic Chemistry 31: 634-639.
4. Baba A, Kawamura N, Makino H, Ohta Y, Taketomi S, et al. (1996) Studies on disease-modifying antirheumatic drugs: Synthesis of novel quinoline and quinazoline derivatives and their anti-inflammatory effect 1. Journal of medicinal chemistry 39: 5176-5182.
5. Kadin SB (1978) 1-oxo-6-substituted pyrimido [1, 2-a] quinoline-2-carboxylic acids and derivatives thereof and their use as antiallergy agents. Google Patents US4066766 A, USA.
6. Tai Y, Landesman Y, Acharya C, Calle Y, Zhong M, at al. (2014) Crm1 inhibition induces tumor cell cytotoxicity and impairs osteoclastogenesis in multiple myeloma: Molecular mechanisms and therapeutic implications. Leukemia 28: 155-165.
7. Sun Q, Carrasco YP, Hu Y, Guo X, Mirzaei H, et al. (2013) Nuclear export inhibition through covalent conjugation and hydrolysis of leptomycin b by crm1. Proceedings of the National Academy of Sciences 110: 1303-1308.
8. Bano S, Alam MS, Javed K, Dudeja M, Das AK, et al. (2015) Synthesis, biological evaluation and molecular docking of some substituted pyrazolines and isoxazolines as potential antimicrobial agents. European journal of medicinal chemistry 95: 96-103.
9. Momose Y, Maekawa T, Yamano T, Kawada M, Odaka H, et al. (2002) Novel 5-substituted 2, 4-thiazolidinedione and 2, 4-oxazolidinedione derivatives as insulin sensitizers with antidiabetic activities. Journal of medicinal chemistry 45: 1518-1534.
10. Etchin J, Sanda T, Mansour MR, Kentsis A, Montero J, et al. (2013) Kpt-330 inhibitor of crm1 (xpo1)-mediated nuclear export has selective anti-leukaemic activity in preclinical models of t-cell acute lymphoblastic leukaemia and acute myeloid leukaemia. British journal of haematology 161: 117-127.
11. Zhang K, Wang M, Tamayo AT, Shacham S, Kauffman M, et al. (2013) Novel selective inhibitors of nuclear export crm1 antagonists for therapy in mantle cell lymphoma. Experimental hematology 41: 67-78.
12. Pearce BC, Wright JJ (1995) Antihyperlipidemic/antioxidant dihydroquinolines. Google Patents US5411969 A, Bristol-Myers Squibb Company, USA.
13. Muruganantham N, Sivakumar R, Anbalagan N, Gunasekaran V, Leonard JT (2004) Synthesis, anticonvulsant and antihypertensive activities of 8-substituted quinoline derivatives. Biological and Pharmaceutical Bulletin 27: 1683-1687.
14. Edmont D, Rocher R, Plisson C, Chenault J (2000) Synthesis and evaluation of quinoline carboxyguanidines as antidiabetic agents. Bioorganic and medicinal chemistry letters 10: 1831-1834.
15. Katsuhik H, Kiyoshi OF (1980) 4-phenyl-2-(1-piperazinyl) quinolines with potent antidepressant activity. Chem Pharm Bull 28: 2618-2622.
16. Sridhar R, Perumal PT, Etti S, Shanmugam G, Ponnuswamy MN, et al. (2004) Design, synthesis and anti-microbial activity of 1h-pyrazole carboxylates. Bioorganic and medicinal chemistry letters 14: 6035-6040.
17. Musad EA, Mohamed R, Saeed BA, Vishwanath BS, Rai LK (2011) Synthesis and evaluation of antioxidant and antibacterial activities of new substituted bis (1, 3, 4-oxadiazoles), 3, 5-bis (substituted) pyrazoles and isoxazoles. Bioorganic and medicinal chemistry letters 21: 3536-3540.
18. Giske CG, Cornaglia G, Goar ES (2010) Surveillance; Supranational surveillance of antimicrobial resistance: The legacy of the last decade and proposals for the future. Drug Resistance Updates 13: 93-98.
19. Rodriguez G (1999) A cohort study on the risk of acute liver injury among users of ketoconazole and other antifungal drugs. British journal of clinical pharmacology 48: 847-852.
20. Legendre DP, Muzny CA, Marshall GD, Swiatlo E (2013) Antibiotic hypersensitivity reactions and approaches to desensitization. Clinical infectious diseases, p: 949.
21. Beasley RP, Lin CC, Hwang LY, Chien CS (1981) Hepatocellular carcinoma and hepatitis b virus: A prospective study of 22 707 men in Taiwan. The Lancet 318: 1129-1133.
22. Zhang W, Koehler K, Zhang P, Cook J (1995) Development of a comprehensive pharmacophore model for the benzodiazepine receptor. Drug design and discovery 12: 193-248.
23. He X, Zhang C, Cook J (2001) Model of the bzr binding site: Correlation of data from site-directed mutagenesis and the pharmacophore/receptor model. Medicinal Chemistry Research 10: 269-308.
24. Saker L, Lee K, Cannito B, Gilmore A, Campbell-Lendrum HD (2004) Globalization and infectious diseases: A review of the linkages. WHO special programme for Research, Switzerland, pp: 1-67.
25. Eswaran S, Adhikari AV, Shetty NS (2009) Synthesis and antimicrobial activities of novel quinoline derivatives carrying 1, 2, 4-triazole moiety. European journal of medicinal chemistry 44: 4637-4647.
26. Narender P, Srinivas U, Ravinder M, Rao BA, Ramesh C, et al. (2006) Synthesis of multisubstituted quinolines from baylis–hillman adducts obtained from substituted 2-chloronicotinaldehydes and their antimicrobial activity. Bioorganic & medicinal chemistry 14: 4600-4609.
27. Koyama K, Ominato K, Natori S, Tashirot T, Tsuruo T (1988) Cytotoxicity and antitumor activities of fungal bis (naphtho-. Gamma. -pyrone) derivatives. Journal of pharmacobio-dynamics 11: 630-635.
28. Koyamas K, Natori N (1987) Chaetochromins b, c and d, bis (naphtho-. Gamma. -pyrone) derivatives from chaetomium gracile. Chemical and pharmaceutical bulletin 35: 578-584.
29. Hou T, Wang J, Li Y, Wang W (2011) Assessing the performance of the mm/pbsa and mm/gbsa methods. 1. The accuracy of binding free energy calculations based on molecular dynamics simulations. Journal of chemical information and modeling 51: 69-82.
30. Khanna S, Bahal R, Bharatam VP (2006) In silico studies on pparγ agonistic heterocyclic systems. In QSAR and molecular modeling studies in heterocyclic drugs. Topics in Heterocyclic Chemistry, India, pp: 149-180.